RXTE Observation of Cygnus X-1: Spectra and Timing

J. Wilms*, J. Dove†, M. Nowak†, B. A. Vaughan‡

*IAA Tübingen, Astronomie, Waldhäuser Str. 64, D-72076 Tübingen
†JILA, University of Colorado, Campus Box 440, Boulder, CO 80309-0440
‡ Space Radiation Laboratory, Caltech, Pasadena, CA 91125

Abstract. We present preliminary results from the analysis of an RXTE observation of Cyg X-1 in the hard state. We show that the observed X-ray spectrum can be explained with a model for an accretion disk corona (ADC), in which a hot sphere is situated inside of a cold accretion disk (similar to an advection dominated model). ADC Models with a slab-geometry do not successfully fit the data. In addition to the spectral results we present the observed temporal properties of Cyg X-1, i.e. the coherence-function and the time-lags, and discuss the constraints the temporal properties imply for the accretion geometry in Cyg X-1.

INTRODUCTION

Cyg X-1 is one of the most firmly established persistent galactic black hole candidates (BHCs). Its X-ray spectrum in the hard state can be described by a power-law with a photon-index $\Gamma \approx (1.5- 1.7)$, modified by an exponential cutoff with a folding energy $E_{\rm fold} \approx 150\,{\rm keV}$ [1,2] and reprocessing features below 10 keV. This spectral form has generally been interpreted as being due to an accretion disk corona (ADC).

As it has been previously pointed out, the standard "slab-like" ADC has problems explaining the high-energy radiation of BHCs, since 1. the strength of the observed reflection component is too small to be consistent with a slab geometry [2], 2. the observed temporal characteristics of Cyg X-1 cannot be explained with a pure slab-like ADC [3], and, 3., numerical models show that the spectral parameters of Cyg X-1 are inconsistent with those predicted for slab-like ADCs [4,5].

In this paper, we use ADC spectra computed using a non-linear Monte Carlo code to model the observed spectrum of Cyg X-1. In addition, we present the global temporal characteristics of Cyg X-1. The results are based on 10 ksec of data from Cyg X-1 obtained with the Rossi X-ray Timing Explorer (RXTE) on October 23, 1996. The data were reduced with ftools 4.0, using version 2.6.1

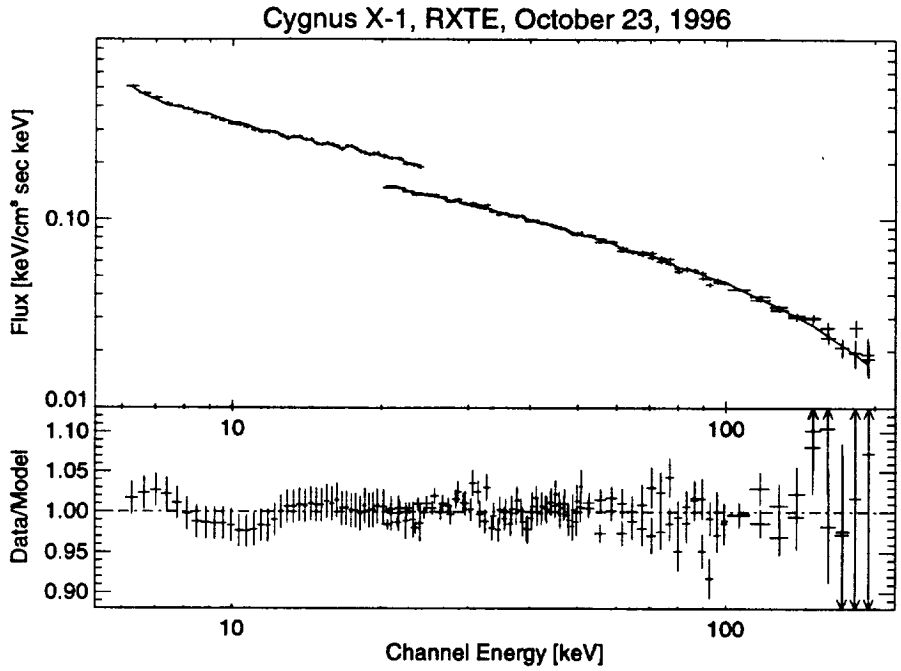

FIGURE 1. Spectrum of the best-fit sphere+disk model, and the ratio between the data and the best-fit model. The jump between the low-energy and the high-energy spectra is due to the uncertainty in the absolute effective areas of the instruments. The relative normalization between the HEXTE clusters and PCA is 0.70 in this fit.

of the PCA response matrix, version 1.5 of the PCA background-estimator program, and the HEXTE response matrices dated March 20, 1997. Due to the uncertainy in the response matrix we model the spectrum between 6 and 200 keV only and add a systematic error of 2% to the PCA data.

SPECTRAL FITTING

Spectral fitting of the RXTE data shows that the spectrum can be well described with a model of the form $KE^{-\Gamma}\exp(-E/E_{\rm f})$, where $\Gamma = 1.4$ and $E_{\rm f} = 150\,{\rm keV}$, *plus* an additional black-body with a temperature of $(1.0 \pm 0.1)\,{\rm keV}$. Since we are ignoring the spectrum below 6 keV the constraint on the temperature of the soft-excess is fairly weak. There is evidence only for a weak reflection component in the spectrum, with the covering factor being $< 0.1 \cdot \Omega/2\pi$.

We have computed grids of spectra for self-consistent ADC models using a non-linear Monte Carlo scheme based on the code of Stern et al. [6] and further described in [4,5]. We have written interpolation routines that enable us to fit the observational data with the data reduction software XSPEC [7]. The data and subroutines are available upon request.

Modeling with spectra from a standard slab-corona, where the accretion disk is embedded between two hot ADCs, does not result in an acceptable fit. Due to the large covering fraction of the cold disk, a large amount of the coronal radiation is reprocessed in the cold disk, resulting in a large flux of thermal radiation which can effectively Compton-cool the corona. Therefore, the temperature of the slab ADCs cannot get high enough to produce a hard spectrum. Slab-models also have too strong of a soft-excess [4]. In contrast, the sphere+disk model, in which a spherical corona is situated at the center of a cold accretion disk, is able to explain the observed spectrum. In Fig. 1 we show the best-fit obtained with the sphere+disk model, as well as the ratio between the data and the best-fit. The seed optical depth of the corona is $\tau_e = 2.1 \pm 0.1$ and the temperature of the corona is $T = 65.7 \pm 3.3\,\mathrm{keV}$. The deviation between the model and the data is always less than 2%, which is an indication that the model is fitting the data quite well. Our formal χ^2_{red}-value for this fit is 1.0. Note that the χ^2-value is affected by the statistical errors associated with Monte Carlo models, where computational time constraints prohibit the generation of models with a very high signal to noise ratio.

TEMPORAL PROPERTIES

Although there is good evidence from the spectral observations that the accretion geometry in Cyg X-1 differs from a simple slab, the results do not rule out other geometries in which the covering fraction of the cold material is smaller than 30%. In order to further constrain the geometry we must consider the temporal properties of the source. For example, since in Comptonization the hard photons emerging from the source will have, on average, undergone more scatterings than low energy photons, there is a time-lag between hard and soft X-rays. The exact form of this time-lag can, in principle, be used to further constrain the accretion geometry of the system. Only a geometry in which both, the spectral *and* the temporal data, can be explained, should be considered a valid candidate geometry for Cyg X-1 [8,9].

Much of the information on the geometry can be obtained by interpreting the phase information of the observed light curve [8,9]. In Fig. 2 we display the coherence between the energy band above 14.9 keVand the energy band below 5 keV. The coherence-function for the frequency f is defined as [8]

$$\gamma^2(f) = \frac{|<C(f)>|^2}{<|S_1(f)|^2><|S_2(f)|^2>}$$

where $C(f)$ is the cross-spectrum between the intrinsic signals $S_i(f) = X_i(f) - N_i(f)$ where $X_i(f)$ is the observed signal and $N_i(f)$ is the Poisson noise-component ("observational rms noise"). The measured coherence of unity from 0.01 Hz to 10 Hz indicates a remarkable stability in the timing properties of the signal over the whole spectrum — an indication that either

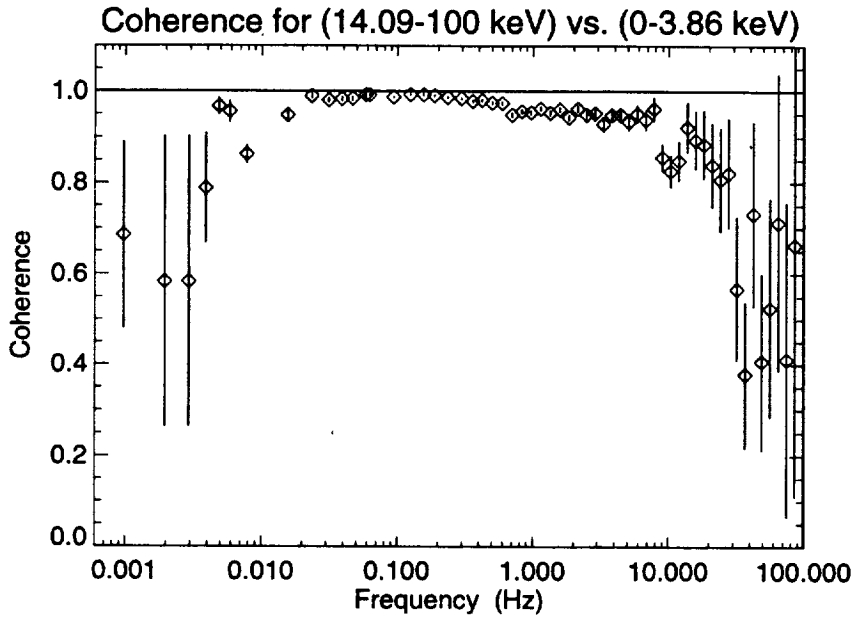

FIGURE 2. Coherence between the hard and soft energies.

there is a single global source for the observed fluctuations, or that there is a global coherent response from the Compton corona, or both [3].

Similar information is also contained in Fig. 3, where the time-lag between the same energy bands is shown. In regions where the coherence function is unity, i.e., 0.01 Hz to 10 Hz, the time-lag can be well determined. Above $\approx$10 Hz the coherence is not preserved and, Poisson noise begins to dominate; therefore, the time-lag varies erratically.

Summary

We have, for the first time, fit the RXTE spectrum of Cyg X-1 using self-consistent ADC models. We have shown that the slab-geometry does not explain the spectrum of the object, while the sphere+disk model, having a smaller covering factor, *can* describe the observed spectrum. In addition, we have presented the measured coherence function and time-lags, which can be used to further constrain the accretion geometry. We emphasize that only the direct application of the models to the observational data can show whether a given geometry is applicable, or not.

We acknowledge helpful discussions with M. Begelman, D. Gruber, I. Kreykenbohm, K. Pottschmidt, Ch. Reynolds, and R. Staubert. This work has been financed by NSF grants AST91-20599, AST95-29175, INT95-13899, NASA Grant NAG5-2025, NAG5-3225, NAG5-3310, DARA grant 50 OR 92054, and by a travel grant to J.W. from the DAAD.

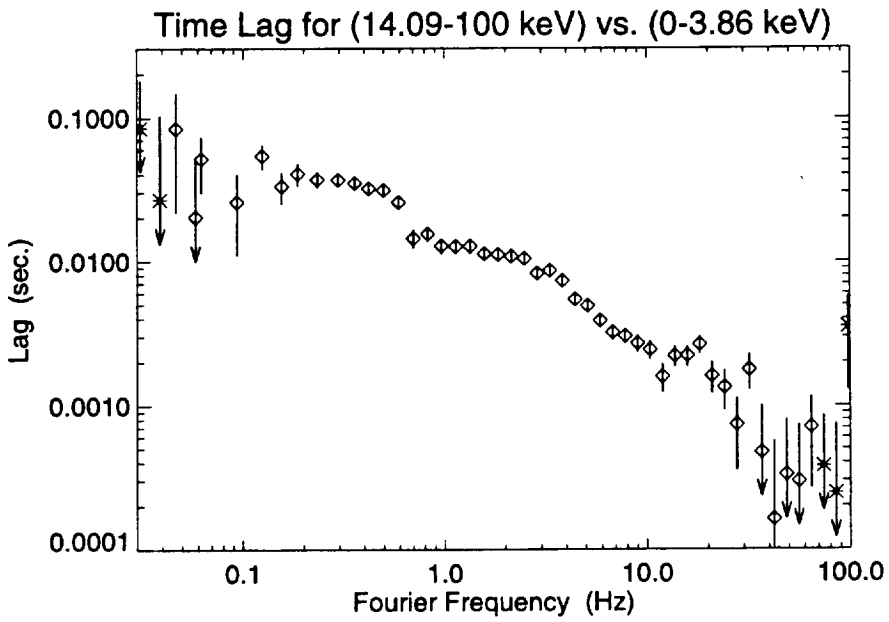

FIGURE 3. Time lag measured between the hard and the soft energy band. Stars indicate a negative time lag, i.e. the hard band leads the soft band. The minimum observed time lags of < 1 ms indicates a maximum coronal size of $< \mathcal{O}(50GM/c^2)$ for $M = 10M_\odot$. The maximum observed time lag constrains the dynamics of the corona.

REFERENCES

1. K. Ebisawa, 1997, Adv. Space Res. **19**, 5.
2. M. Gierliński et al., 1997, MNRAS, in press.
3. M. A. Nowak, B. A. Vaughan, J. Dove, and J. Wilms, 1997, IAU Coll. 163, in press
4. J. B. Dove, J. Wilms, and M. C. Begelman, 1997, ApJ **487**, in press (October 1, 1997, issue).
5. J. B. Dove, J. Wilms, M. G. Maisack, and M. C. Begelman, 1997, ApJ **487** (1997) in press (October 1, 1997, issue).
6. B. E. Stern, M. C. Begelman, M. Sikora, and R. Svensson, MNRAS **272**, 291 (1995).
7. K. A. Arnaud, 1996, in ADASS V, J. H. Jacoby and J. Barnes (eds.), ASP Conf. Ser., 101, San Francisco: Astron. Soc. Pacific., 17
8. B. A. Vaughan and M. A. Nowak, 1997, ApJ **474**, L43.
9. M. A. Nowak and B. A. Vaughan, 1996, MNRAS **280**, 227.

RXTE Observation of Cygnus X-1: Spectral Analysis

J. B. Dove[a], Jörn Wilms[b], M. A. Nowak[c], Brian Vaughan[d] and M. C. Begelman[e*]

[a]Department of Physics and Astronomy, University of Wyoming, Laramie, WY 82071

[b]Institut für Astronomie und Astrophysik, Abt. Astronomie, Waldhäuser Str. 64, D-72076 Tübingen, Germany

[c]JILA, University of Colorado and the National Institue of Standards and Technology, Campus Box 440, Boulder, CO 80309

[d]Space Radiation Laboratory, California Institute of Technology, 220-47 Downs, Pasadena, CA 91125

[e]JILA, University of Colorado and National Institute of Standards and Technology, Campus Box 440,Boulder, CO 80309

We present the results of the analysis of the broad-band spectrum of Cygnus X-1 from 3.0 to 200 keV, using data from a 10 ksec observation by the *Rossi X-ray Timing Explorer*. Although the spectrum can be well described phenomenologically by an exponentially cut-off power law (photon index $\Gamma = 1.45^{+0.01}_{-0.02}$, e-folding energy $E_f = 162^{+9}_{-8}$ keV, plus a deviation from a power law that formally can be modeled as a thermal blackbody with temperature $kT_{BB} = 1.2^{+0.0}_{-0.1}$ keV), the inclusion of a reflection component does *not* improve the fit. As a physical description of this system, we apply the accretion disc corona models of Dove, Wilms & Begelman [4] — where the temperature of the corona is determined self-consistently. A spherical corona with a total optical depth $\tau = 1.6 \pm 0.1$ and an average temperature $kT_C = 87 \pm 5$ keV, surrounded by an exterior cold disc, does provide a good description of the data ($\chi^2_{red} = 1.55$). These models deviate from the data by up to 7% in the 5–10 keV range, and we discuss possible reasons for these discrepancies. However, considering how successfully the spherical corona reproduces the 10–200 keV data, such "photon-starved" coronal geometries seem very promising for explaining the accretion processes of Cygnus X-1.

1. Introduction

Cygnus X-1 is one of the most firmly established persistent galactic black hole candidates (BHCs). The combination of a Comptonization continuum and reprocessing features has been interpreted as being due to an accretion disc corona (ADC). The geometric configuration of the corona and the cold disc, however, is still unclear. In most prior work, the geometry has been assumed to be a cold accretion disc embedded between two hot coronae, with a slab geometry [10,9].Recently, however, evidence has been presented showing that ADC models with a slab geometry suffer from several problems, making them less likely to be the appropriate models for explaining the high-energy radiation of BHCs. Gierliński et al. [8] analyzed simultaneous *Ginga*-OSSE data of Cyg X-1 and found that the strength of the reflection component is too small to be consistent with a slab geometry. Using a non-simultaneous broad-band spectrum of Cyg X-1, we previously argued that our self-consistent ADC models with a slab geometry (in which the coronal temperature is not a free parameter but is determined by balancing Comp-

*This work has been financed by NSF grants AST91-20599, AST95-29175, INT95-13899, NASA Grant NAG5-2026, NAG5-3225, NAGS-3310, DARA grant 50 OR 92054, and by a travel grant to J.W. from the DAAD.

ton cooling with viscous dissipation) could not have a high enough temperature to explain both the observed power-law and exponential cutoff [4,5].

In this paper, we analyze the broad-band spectrum of Cyg X-1 from 3.0 to 200 keV, using data from the *Rossi X-ray Timing Explorer* (RXTE). The simultaneity of this broad-band observation allows us to place stronger constraints on the coronal parameters than previously possible. In §2, we give the results from spectral modeling of the Cyg X-1 spectrum using both "standard" simplified models as well as our self-consistent ADC models. In §3 the results of these fits are discussed.

2. Spectral Analysis

RXTE observed Cyg X-1 for a total of 22.5 ksec on 1996 October 23 and 24. For the analysis presented here, we use data from the proportional counter array (PCA) and the high energy X-ray timing experiment (HEXTE).

2.1. Standard Models

Spectral fitting was first performed using the following standard models: a power-law, a power-law with an exponential cutoff, a power-law with an exponential cutoff plus a cold reflection component, and thermal Comptonization models. In addition, we added a Gaussian line (with energy and width fixed to 6.4 keV and 0.1 keV, respectively) to several of these models. We fixed the low-energy absorption to an equivalent cold Hydrogen column of $N_{\rm H} = 6 \times 10^{21}\,{\rm cm}^{-2}$, the value suggested by the soft X-ray spectrum and interstellar reddening measurements of HDE 226868 [1,14]. For energies $E \gtrsim 10$ keV, a power-law with an exponential cutoff provides a good description of the data, as also shown in Figure 1. The value for the e-folding energy, $E_{\rm f}$, is well constrained due to the quality of the HEXTE data. The analysis of the residuals of this fit indicates the presence of a soft excess at energies $\lesssim 8$ keV, as shown in Figure 1. Adding a black-body component with

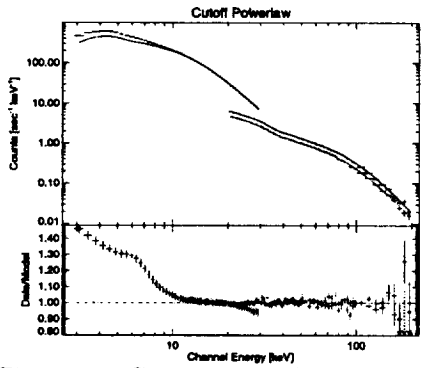

Figure 1. Comparison of the RXTE spectrum of Cyg X-1 to the best-fit power-law with an exponential cutoff model. This model was fit to only the 10–200 keV data. The photon power-law index $\Gamma = 1.46$ and the e-folding energy $E_{\rm f} = 167$ keV. A soft-excess below 10 keV is clearly evident.

a temperature $kT_{\rm BB} \approx 1$ keV and a Gaussian component, with an equivalent width EW= 46.4 eV, to the model improves the quality of the fit, resulting in a good description of the data over the whole energy range ($\chi^2_{\rm red} = 169/166$), as shown in Figure 2. We note that this black-body component should not be interpreted literally as being due to disc emission: it is simply added phenomenologically to measure the magnitude of the data's deviation from a power law. We could have instead used a disc blackbody, Gaussian, or bremsstrahlung model with roughly equal success.

The addition of a reflection component to this model *does not* improve the quality of the fit, as the best-fit value for the fraction of incident radiation that is Compton reflected by cold matter is $f \lesssim 0.02$. Even though we only considered PCA data between 3.0 keV and 30 keV, the power-law index of the continuum is well constrained by the HEXTE data, and there is no evidence that the spectral slope of the data for the two instruments disagree within the energy range of the overlap. The PCA residuals between 20 and 30 keV seen in Figure 1-4 are consistent with those seen

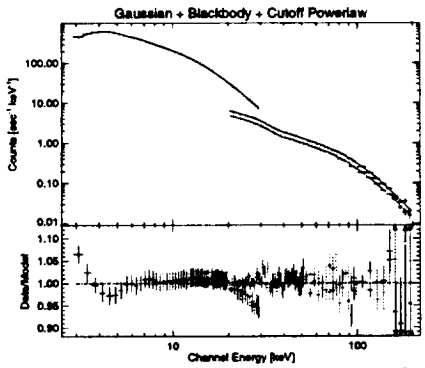

Figure 2. Comparison of the RXTE spectrum of Cyg X-1 to the best-fit power-law with an exponential cutoff model. The photon power-law index $\Gamma = 1.45$ and the e-folding energy is $E_f = 163\,\mathrm{keV}$. A blackbody component, with a temperature $kT_{BB} = 1.1\,\mathrm{keV}$ and a relative flux of $\lesssim 5\%$, and a Gaussian component, with an energy fixed at 6.4 keV and an equivalent width EW= 46.4 eV, were added to fit the soft-excess. For this fit, $\chi^2_{red} = 169/166$.

for power-law fits to the Crab.

It is this 30–100 keV energy range that is crucial for constraining a power-law index since these energies are uncontaminated by reprocessing or reflection features. We therefore postulate that the observed 10–30 keV "hardening" feature typically found by others appears to be the beginning of a hard power-law that continues to $\sim$ 100 keV, and that the $\sim$ 1–10 keV portion of the spectrum has a softer power-law due to contamination from the thermal excess. This contamination could be due to Comptonization of the thermal radiation emitted by the cold disk with an effective blackbody temperature $kT_{BB} \sim 150\,\mathrm{keV}$, since, for energies $\lesssim 10kT_{BB}$, the Comptonized spectrum is not expected to be a power law.

We believe that the measured spectrum parameters, which represent a harder power law and a weaker reflection component than previously found by others, is mostly due to our fitting the entire 3–200 keV spectral band. Previous observations using different instruments have had relatively poor spectral coverage between $\sim$ 30–100 keV. results are heavily influenced by any remaining uncertainties in the PCA response matrix. To support this claim, if we restrict the data to 3–30 keV we *do* find best-fit parameter values similar to those previously found for Cyg X-1. Specifically, for this restricted data range, we find that a reflected power law with $\Gamma = 1.81 \pm 0.01$ and covering fraction $f = 0.35 \pm 0.02$ yields $\chi^2_{red} = 157/90 = 1.75$. Adding back the HEXTE data in the 30–100 keV range significantly reduces the quality of the fit ($\chi^2_{red} = 8.7$, 77 dof). Therefore, being able to fit a reflected power-law with a large disk covering fraction is seen to be partly a consequence of ignoring the data in the $\sim$ 30–100 keV range. We refer the reader to our forthcoming paper [6] for a more detailed discussion of this issue.

2.2. Accretion Disc Corona models

For both a slab ADC model and the sphere+disc ADC model, we have computed grids of spectra using a non-linear Monte Carlo scheme based on the code of Stern et al. [13] and modified by Dove et al. [4] and Dove et al. [5]. Slab-corona models do not result in good fits, as the predicted spectra are always much softer than the observed spectrum ($\chi^2_{red} \sim 80$). This result is consistent with our previous findings based on non-simultaneous data [5].

The sphere+disk ADC model does provide a good description to the data (cf. table ?? and figure 3). The formal χ^2-value of our best-fit model ($\chi^2_{red} = 1.55$) is larger than the values found for some of the phenomenological models discussed in §3.1. Considering that our model has only three parameters (seed optical depth, coronal compactness, overall normalization, plus the "hidden" parameter T_{BB}, which is fixed at 150 eV during the fitting procedure), and considering that our model is ***physically self-consistent***, the level of

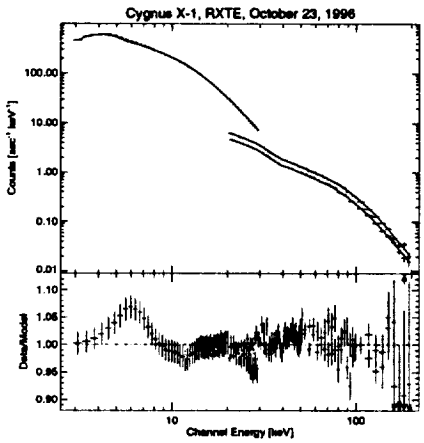

Figure 3. Top: Best-fit sphere+disc fit to the PCA and HEXTE data. Bottom: Ratio between data and model for the best-fit sphere+disc model. Deviations less than 2% are within the range of uncertainty of the PCA response matrix. Deviations in the 20-30 keV range are similar to those seen with best-fit models of Crab nebula observations (Jahoda 1997, private communication).

agreement with the data is quite good. The major disagreement between the model and the data occurs in the $\approx$ 5–10 keV range, where the residuals are as large as 7%.

3. Conclusions

We have applied a variety of spectral models to an RXTE observation of Cyg X-1. We find that the observed spectrum between 3.0 and 200 keV is well described by a power-law with a photon index $\Gamma = 1.45^{+0.01}_{-0.02}$ modified by an exponential tail with an e-folding energy $E_f \approx 160$ keV, and a soft excess that was modeled as a black-body (although other broad distribution models are capable of explaining the soft-excess) having a temperature $kT_{\rm BB} \approx 1.2$ keV. The measured value of Γ is lower than those found in previous broad-band analyses, which find a $\Gamma \sim 1.65$ [8,3]. In addition, the observed strength of the Compton reflection feature is weak, as the best-fit covering fraction, determined by fitting the data with a power-law reflection model [11], is found to be ≈ 0.2 when no soft excess component is included, and is found to be $\lesssim 0.02$ when one is included. The latter value is considerably lower than the $f \approx 0.3$ found by Gierliński et al. [8]. The sphere+disc ADC models provide a good explanation of the data, and furthermore these models are *physically self-consistent.* For a more detailed discussion of these results, we refer the reader to Dove et al. [6].

REFERENCES

1. Bałucińska, M., & Hasinger, G., 1991, A&A, 241, 439
2. Barr, P., White, N. E., & Page, C. G., 1985, MNRAS, 216, 65p
3. Döbereiner, S., et al., 1994, A&A, 287, 105
4. Dove, J. B., Wilms, J., & Begelman, M. C., 1997, ApJ, 487, 747
5. Dove, J. B., Wilms, J., Maisack, M. G., & Begelman, M. C., 1997, ApJ, 487, 759
6. Dove, J. B., Wilms, M. A. Nowak, B. A. Vaughan, M. G., & Begelman, M. C., 1997, MNRAS, submitted
7. Ebisawa, K., Ueda, Y., Inoue, H., Tanaka, Y., & White, N. E., 1996, ApJ, 467, 419
8. Gierliński, M., Zdziarski, A. A., Done, C., Johnson, W. N., Ebisawa, K., Ueda, Y., Haardt, F., & Phlips, B. F., 1997, MNRAS, 288, 958
9. Haardt, F., Done, C., Matt, G., & Fabian, A. C., 1993, ApJ, 411, L95
10. Haardt, F., Maraschi, L., & Ghisellini, G., 1996, ApJ, 476, 670
11. Magdziarz, P., & Zdziarski, A. A., 1995, MNRAS, 273, 837
12. Poutanen, J., Krolik, J. H., & Ryde, F., 1997, MNRAS, submitted
13. Stern, B. E., Begelman, M. C., Sikora, M., & Svensson, R., 1995, MNRAS, 272, 291
14. Wu, C.-C., Eaton, J. A., Holm, A. V., Milgrom, M., & Hammer-